# Effects of Plasma Radiation on the Thomson Scattering Diagnostic Installed on the Large Helical Device

Kazumichi NARIHARA, Ichihiro YAMADA, Hiroshi HAYASHI and Hisamichi FUNABA

*National Institute for Fusion Science, Toki 509-5292, Japan*

Recently we modified the Thomson scattering diagnostic (TS) installed on LHD so that DC levels ($V_{DC}$) of all avalanche photodiodes (APD) used for detecting scattered light can be registered every 1 ms, which enabling us to make validity check on TS data taken under very intense plasma radiation. In the line of this task, we first examined how the pulse-performance of an APD degrades as the intensity of continuous light ($J_{DC}$) incident to the APD increases. We found two effects are involved in deteriorating the pulse-performance of the APD: (1) the responsivity of the APD to a pulsed light drops as $J_{DC}$ increases, causing a systematic errors on the deduced electron temperature ($T_e$) and density ($n_e$); (2) the frequency response of the APD and the following circuit drops as $J_{DC}$ increases, which deforms the pulse shape. The bias voltage applied to the APD ($V_b$) has large influence on these behaviors, showing the best overall performance for a high $J_{DC}$ around $V_b \sim 0.5 V_r$, where $V_r$ is the recommended voltage giving responsivity of 675 kV/W at 1060 nm. Considering these effects together, we set a conservative validity criterion for the pulse APD performance in term of the $V_{DC}$: $V_{DC} < 0.5$ V. The $V_b = 0.5 V_r$ setup gives much reliable $T_e$-profiles without a collapse in $T_e$-profile for a much wider range of plasma radiation intensity. With this criterion, we check the validity of $T_e$-and $n_e$-profiles of two example data.

## 1. Introduction

Thomson scattering diagnostic (TS) is widely used for measuring electron temperature ($T_e$) and density ($n_e$) in fusion plasma experiments because of its high reliability. However, this 'reliability', is realized only in a limited ranges of plasma- and setting- parameters and through a careful calibration. We should make a severe validity check on TS data as the plasma to be measured enters a new regime such as the very high-density plasma which was recently observed [1]. In applying TS to very dense plasma, the first thing to be checked is the 'incoherence scattering' condition: the wavelength associated with the momentum transfer $\lambda = \lambda_L/2\sin(\theta/2)$ should be less than the Debye length. With $\lambda_L = 1.06 \mu m$ (Nd:YAG laser) and $\sin(\theta/2)\sim 1$ for the LHD-TS configuration this condition is expressed as $(n_e/10^{20}\text{m}^{-3})/(T_e/\text{keV}) < 10^5$, which is sufficiently met even in the low temperature edge region with $T_e \sim 20$ eV. Another concern is the effect of intense plasma radiation on the pulse-performance of avalanche photo diodes (APD) used for detecting scattered light, since as $n_e$ goes up the plasma Bremsstrahlung increases in proportion to $n_e^2$ [2], while the scattered signal in proportional to $n_e$. To solve this problem to some extent by monitoring the DC-level of each APD output, which is supposed to be proportional to the intensity of plasma radiation, we modified the existing LHD-TS and implemented scanning ADCs. This

paper treats this plasma radiation problem. The next section describes the LHD-TS and its modification, Section 3 shows the measured pulse-performance of an APD under an intense continuous light illumination, Section 4 examines validity of $T_e$ and $n_e$ profiles of two example shots, and Section 5 gives discussions.

## 2. LHD Thomson Scattering Diagnostic

We first give a very brief description on the LHD-TS [3,4] and the modification done recently. The LHD-TS is characterized by its heavily inclined backward scattering configuration, which enables measuring $T_e$ and density $n_e$ at 200 points along a major radius passing the magnetic axis, covering entire region from the inner- to outer-edges of the plasma. Three 2J-10 Hz Nd:YAG lasers give $T_e$ and $n_e$ profiles at 30 Hz repetition rate. The scattered light from each scattering volume is collected on a tip of 200 optical fibers of 2 mm in diameter and transported 45 m to a five-color filter polychromator, where it is resolved into five spectra, each of which is detected by an APD (EG&G C30950 CD-1161). A diagram of the APD circuit plus data acquisition system is shown in Fig. 1. To each APD the bias voltage ($V_b$) equal to 0.9 times the recommended voltage ($V_r$) which gives the responsivity $R = 675$ kV/W at 1060 nm is applied through a 100 kΩ resistor. This resistor is absolutely necessary for guarding the APD and
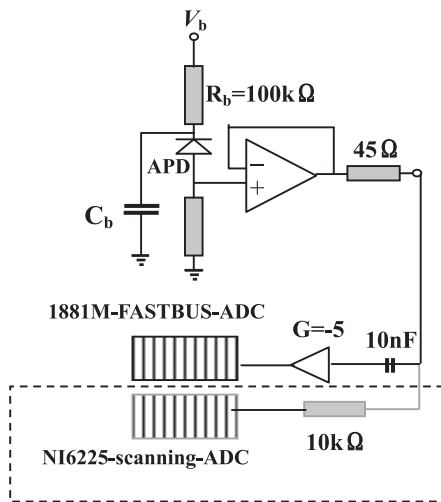
Fig. 1   Schematic drawing of the APD plus data acquisition system. The lower part enclosed by dashed line is newly installed.



Fig. 2   DC output voltages as a function of $V_b$ for $R_b = 0\,k\Omega$ and $100\,k\Omega$. Continuous light intensity was held at a constant.



Fig. 3   Amplitude of 30ns-pulse-signal as a function of $V_{DC}$ for $V_b = 0.9\,V_r$ and $V_b = 0.5\,V_r$ settings. Note that input light intensity is not exactly the same for the two measurements.

the following circuit against damage due to excess light illumination with a long duration. For a very short pulse light illumination such as TS light, the capacitor $C_b$ will supply enough charge at a constant voltage. The output of APD is connected to an inverting wideband amplifier with gain g~5 via a capacitor of 10nF and fed to charge-ADC (Lecroy FASTBUS 1881 M). This capacitor is used to block the low frequency ($f < 1$ MHz) fluctuating plasma light to enter into the signal, thus the information on the DC output of the APD ($V_{DC}$) being lost. Including laser monitor signals, total number of signals to be fed to ADCs is 1024. As the LHD experiment began to explore into a very high-density regime with central $n_e > 10^{20}\text{m}^{-3}$, and hence, the data validity of the TS data being suspected, we modified the LHD-TS so that $V_{DC}$ of all APDs can be monitored routinely. For this aim, we connected the output of each APD to the input of scanning ADC (NI 6225, maximum scanning rate is 1 ms) via $10\,k\Omega$ resistor, which is needed to keep the impedance matching for the short pulse propagation in cables.

## 3. Characteristics of APD under Intense Background Light Illumination

In considering the plasma radiation effects on the performance of an APD for detecting a very short pulse light, important issues are the responsivity ($R$) saturation and the change of frequency response, the latter of which has influence to the former for a pulse light detection. It is reported that an APD itself has a good linearity over many orders of magnitudes of incident light [5]. The $R$ saturation mechanisms in the body of an APD, such as space-charge effect and heating effect were discussed in literatures [5]. Another sources of the $R$ saturation come from an electric circuit used for an APD. Referring to Fig. 1, we guess two
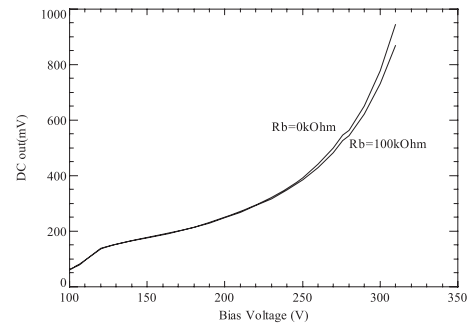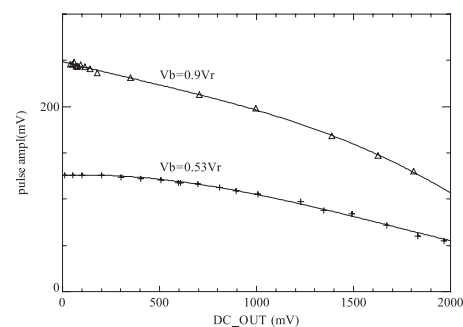
sources of $R$ saturation: (1) one is the voltage drop across the resistor $R_b$ and the consequent $R$ drop; (2) the other is the saturation of output voltage of the amplifier due to a limited current driving capability of the output transistor. In order to examine these guessed effects, we tested a sample APD (EG&G C30950 CD-1161 S/N = C2087-D), whose specifications are: the recommended operating voltage ($V_r$) which gives the responsivity $R = 675\,kV/W$ is 307 V; dark current $I_d = 180$ nA, bandwidth $B = 25$ MHz, and the noise equivalent power $NEP = 60\,fW/\sqrt{Hz}$. We first measured the $V_{DC}$ as a function of $V_r$ for $R_b = 0\,k\Omega$ and $R_b = 100\,k\Omega$ settings under a fixed continuous light illumination from a tungsten lamp. The results are shown in Fig. 2. The curve for $R_b = 0\,k\Omega$ can be regarded as the intrinsic $R$ as a function of $V_b$ apart from some constant: $R = R(V_b)$. The curve for the $R_b = 100\,k\Omega$ setting shows up $R$-drop due to the voltage drop across $R_b$. In order to reduce the $R$-drop due to voltage drop across $R_b$, it is obviously favorable to operate at lower $V_b$, where the derivative of $R(V_b)$ is the smaller. However, lowering $V_b$ leads to an increase of the capacity across the depression layer of the APD, loosing the fast response necessary for detecting short pulse TS light. The allowable minimum $V_b$ for this APD is about 0.5 $V_r$.
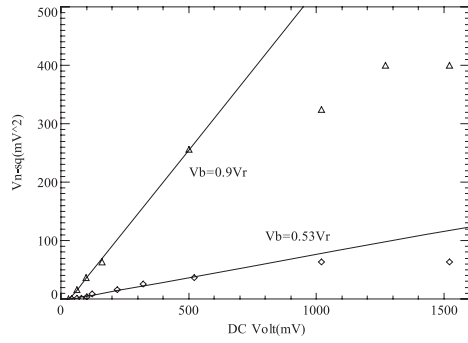
Fig. 4　Square of wide band noise p-p voltage as a function of $V_{DC}$ for $V_b = 0.9V_r$ and $V_b = 0.53\,V_r$.

Secondly, we measured the pulse-output voltage in response to the pulse light as a function of the $V_{DC}$, which was changed by the current in the tungsten lamp, for the fixed bias voltages of $V_b = 0.9\,V_r$ and $V_b = 0.5V_r$, with the results show in Fig. 3. The output pulse height gradually decreases as $V_{DC}$ rises, with the faster decay for the higher $V_b$, which is partly explained by the larger $dR/dV_b$ for the higher $V_b$ as seen in Fig. 2. The drop in pulse amplitude for $V_{DC} > 0.5\,V$ seems to result from the narrowing of the bandwidth ($B$) of the APD plus the following circuit, which is evidenced as a deformation of output pulse shape. To check this observation further, we measured the square of the peak-to-peak voltage ($V_n$) of wideband noise as a function of $V_{DC}$ for $V_b = 0.5\,V_r$ and $0.9\,V_r$ settings. The results are shown in Fig. 4.

According to the noise theory [6], $< V_n^2 >\propto R^2 I_{pe}B \propto R^2 BV_{DC}$. Here $I_{pe}$ is the diode current, which is proportional to $V_{DC}$. This relation holds up to $V_{DC} = 0.5\,V$ for both bias voltages. The departure from the theoretical curve implies that $B$ becomes smaller than needed for pulse-light detection when $V_{DC}$ exceeds $0.5\,V$.

Taking account of the above measured data together, we consider that the pulse-signal from the APD under intense light illumination is valid if $V_{DC} < 0.5\,V$, irrespective of the $V_b$-setting. Under the $V_b = 0.9\,V_r$ setting, $V_{DC}$ reaches $0.5\,V$ with a lower intensity light illumination. Moreover, within this criterion, pulse signals suffer drop in magnitude up to 10 %, introducing the same magnitude errors in the deduced $T_e$ and $n_e$. A correction scheme in a data deduction program using $V_{DC}$ data may reduce these errors substantially. On the other hand, under the $V_b = 0.5\,V_r$ setting, the $V_{DC}$ is below $0.5\,V$ for much intense continuous light illumination without appreciable drop in $R$, thus being much favorable for measuring a very high density plasma, which inevitably accompanies intense plasma radiation.

# 4. Examination of $T_e$-and $n_e$-Profiles

Firstly, we examine the data that yields unnatural $T_e$- and $n_e$-profiles such as shown in Fig. 5 (A). The $V_b$ was
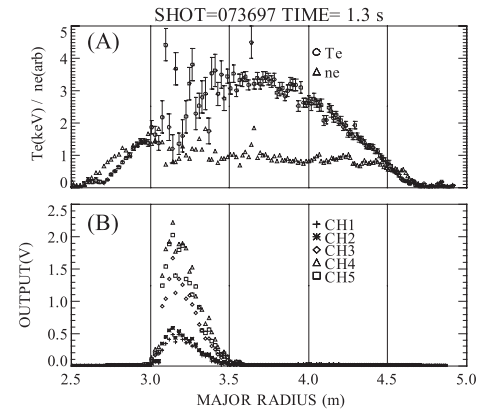


Fig. 5　(A) An example with unnatural $T_e$ and $n_e$ profiles. $V_b = 0.9\,V_r$. (B) Spatial $V_{DC}$-distributions. In order of the magnitude (from the top): ch5, ch4, ch3, ch2 and ch1. The ch1 collects light of the longest wavelength.
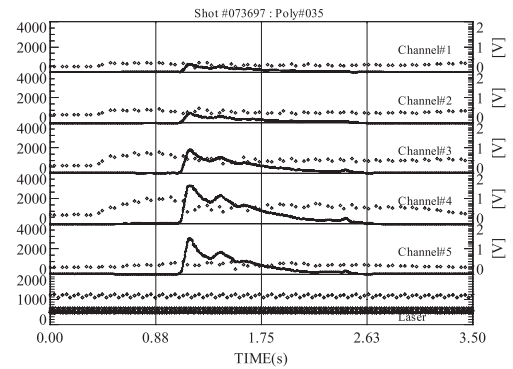


Fig. 6　Time evolutions of five-channel TS-signal and $V_{DC}$ from the #35 polychromator, which 'sees' $R \sim 3.22\,m$. The solid lines (right scale) are $V_{DC}$. The dotted lines are TS-signal (left scale).

set at $0.9\,V_r$. The distribution of $V_{DC}$ at the time when $T_e$-profile was taken is shown in Fig. 5 (B) for five color-channels. We can see that high $V_{DC}$ exceeding $0.5\,V$ localizes around $3.0\,m < R_o$ (major radius)$< 3.4\,m$, where the $T_e$-profile accompanies large error-bars. From our criterion described above, the raw data and hence the deduced $T_e$ and $n_e$ between $3.0\,m < R_o < 3.4\,m$ are invalid.

Examining the TS optical configuration, we confirmed that the polychromators yielding the high $V_{DC}$ 'see' the divertor plates behind.

Figure 6 shows the time evolutions of $V_{DC}$ from the #35polychromator, which 'sees' around $R \sim 3.22\,m$. The $V_{DC}$ rise exceeding the criterion voltage of $0.5\,V$ with $230\,ms$ delay after NB injection (#1+#2+#3). This phenomenon depends on the LHD magnetic configuration and plasma parameters.

The second example is data that yields $T_e$- and $n_e$-profiles shown in Fig. 7 (A). The $V_b$ was set to $0.5\,V_r$. Spatial distributions of $V_{DC}$ are plotted in Fig. 7 (B).

All $V_{DC}$ are small enough to guarantee the validity
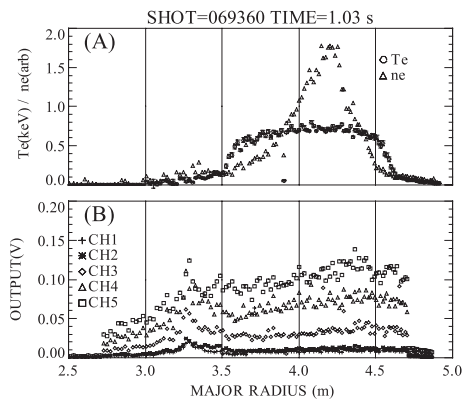
SHOT=069360 TIME=1.03 s

Fig. 7  (A) An example of $T_e$- and $n_e$- profiles. $V_b = 0.5V_r$. (B) Spatial distribution of 5-channel $V_{DC}$. In order of magnitude (from the top), ch5, ch4, ch3, ch2 and ch1.
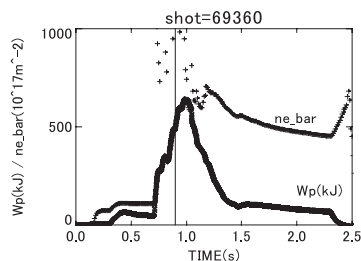


Fig. 8  Time evolutions of line integrated density ($n_{e\_bar}$) and diamagnetic energy ($W_p$).

of the APD pulse-signals. The electron density integrated along the center cord ($n_{e\_bar}$) and the diamagnetic energy ($W_p$) as function of time are shown in Fig. 8. Assuming that the $n_e$ profile is correct and comparing $\int n_e \, dR_o$ with $n_{e\_bar}$ at 0.53 s, when the HCN interferometer data was still free from a fringe-jump, we give the scale for $n_e$ shown in Fig. 8. If we succeed in developing an absolute $n_e$ calibration method based on high-pressure Rayleigh scattering with a much reduced laser power, thus mitigating the severe stray light problem, we may get a more precise and

probably smoother $n_e$ profiles.

Under the $V_b = 0.5 V_r$ setting, most, if not all, of the plasma with the magnetic axis position greater than 3.75 m show that $V_{DC} < 0.5$ V, thus proved to have valid TS-data. If plasma radiation intensity is low enough, the $V_b = 0.9 V_r$ setting is more suitable to obtain better data quality.

## 5. Discussions

We examined the effect of continuous light illumination on the pulse-performance of an APD in terms of the pulse-amplitude and the bandwidth, and offered the validity criterion: $V_{DC} < 0.5$ V. In reality, however, the scattering signals that are converted to digital data and used for data deduction are the time integration of the signal (q-data) over a fixed gate interval (usually 60 ns-100 ns). If the effects are examined in term of the q-data, a somewhat different criterion may be obtained. Moreover, since characteristic of APDs differ appreciably from piece to piece, it is necessary to examine the effects of continuous light illumination on q-data of all 1000-APDs. For this purpose we are preparing a white reflector coated with $BaSO_4$ of 65 cm × 32 cm in area, which is set on the observation window and illuminated by both continuous and pulse light. The diffused light thus obtained will facilitate simultaneous examination of all 1000-APDs.

We adopted scanning ADCs to monitor the DC-levels of all APD for the economical reason, but much better is to use GHz-sampling digitizers that register all information including the shape of the scattered signals and the background plasma radiation as adopted on ASDEX-U [7].

[1] N. Ohyabu *et al.*, Phys. Rev. Lett. **97**, 055002 (2006).
[2] I.H. Hutchinson, *Principles of Plasma Diagnostics* (Cambridge University Press, 1987).
[3] K.Narihara *et al.*, Fusion Eng. Des. **34-35**, 67 (1997).
[4] K. Narihara *et al.*, Rev. Sci. Instrum. **72**, 1122 (2001).
[5] P.P Webb, R.J. Mclntyre and J. Conradi, RCA Review **35**, 234 (1974).
[6] R.E. Simon edited, *Electro-Optics Handbook*, RCA (1974).
[7] B. Kurzan, M. Jakobi, H. Murmann *et al.*, Plasma Phys. Control. Fusion **46**, 299 (2004).